Direct Observation of Twisted Grain Boundary in a Block Copolymer Lamellar Nanostructure†

Hiroshi Jinnai,*,‡ Koji Sawa,‡ and Toshio Nishi§

Department of Macromolecular Science and Engineering, Graduate School of Science and Technology, Kyoto Institute of Technology, Matsugasaki, Kyoto 606-8585, Japan, and Department of Organic and Polymeric Materials, School of Science and Engineering, Tokyo Institute of Technology, 2-12-1, Ohokayama, Meguro-ku, Tokyo 152-8552, Japan

Received January 4, 2006; Revised Manuscript Received May 8, 2006

ABSTRACT: The grain boundary morphology of a lamella-forming poly(styrene-*b*-isoprene) (SI) diblock copolymer was investigated by transmission electron microtomography. The twist grain boundary, at which two lamellar nanodomains orthogonally intersect, was successfully observed in three dimensions (3D). A two-dimensional periodic minimal surface, the Scherk's first surface, was once hypothesized as a model of such a grain boundary morphology but never experimentally ascertained. The area-averaged curvatures of the interface between the PI and PS nanodomains as well as the interfacial area per unit volume suggested that the grain boundary morphology had characteristics of the saddlelike hyperbolic surface and was found to be quite similar to Scherk's first surface.

I. Introduction

Block copolymers often exhibit nanodomain structures with various morphologies.[1,2] The macroscopic properties of such systems depend not only on the local structure in the mesoscopic scale of 10−100 nm but also on the long-range order on a scale of micrometers or larger. The morphology of boundary regions between grains influences the mechanical, electrical, and diffusional properties[3,4] of block copolymer to a great extent.[5−7] Although important, the three-dimensional (3D) continuity of each nanodomain at the grain boundary is not trivial, especially in lamellar and cylindrical structures due to their high orientation and nonequilibrium nature.

The grain boundaries in lamella-forming block copolymers can be divided into two types: the kink (tilt) grain boundary (KGB) and the twist grain boundary (TGB). In the KGB, normals to the lamellae of two neighboring grains establish a plane that is perpendicular to the boundary surface. In the TGB, on the other hand, the plane is parallel to the boundary surface. The KGB of block copolymers has been intensively studied, both experimentally[6,8−10] and theoretically.[11] For example, Gido et al. explored the grain boundary morphologies in poly(styrene-*block*-isoprene) (SI) lamellar diblock copolymers using transmission electron microscopy (TEM).[6] The motion of a KGB in a poly(styrene-*block*-ethylene propylene) lamellar diblock copolymer in the presence of an external shear field was studied by TEM and small-angle X-ray scattering (SAXS).[8−10]

In contrast to the KGB, there are few experimental studies concerning the structure of TGBs in the literature.[5−7] Thomas et al. proposed the doubly periodic morphology approximating Scherk's first surface as a model for high angle TGB in lamellar systems simply due to the minimization of the surface area.[12] Figure 1a demonstrates a model surface of the Scherk's first surface produced by computer graphics using the following equation for Cartesian coordinates (x, y, z).[5]

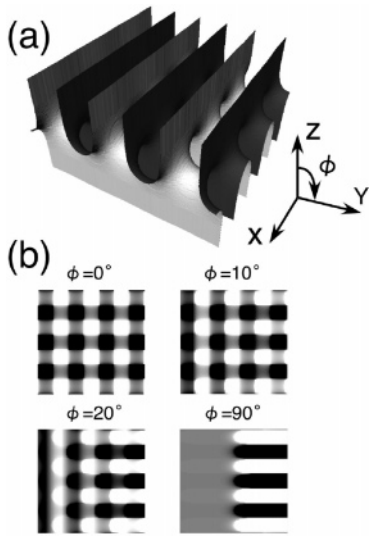

Figure 1. (a) Computer-generated Scherk's first surface. (b) Computer simulation images of ultrathin sections for grain boundaries of lamellar nanodomains with Scherk's first surface as a mathematical model. Uniform staining within one-type domain is assumed, and the section thickness was fixed to one repeat distance of the lamellae. Tilt angle ϕ is defined in (a).

$$\exp z \cos x = \cos y \tag{1}$$

A set of saddlelike hyperbolic surfaces is formed between the two orthogonal sets of parallel planes. On the basis of such a mathematical model, four computer-simulated images are depicted in Figure 1b. These 2D pictures indicate how the Scherk's first surface would appear under the TEM. The simulated image at the top left ($\phi = 0°$) corresponds to projecting directly down the z-axis of the Scherk surface, while the one at the bottom right ($\phi = 90°$) corresponds to projecting down the y-axis. The angle ϕ is defined in Figure 1a. In each simulation, three levels of intensities are presented: The black

† Presented in part at the 230th ACS National Meeting, Aug 28−Sept 1, 2005.

‡ Kyoto Institute of Technology.
§ Tokyo Institute of Technology.
* To whom correspondence should be addressed: e-mail: hjinnai@kit.ac.jp.

10.1021/ma0600153 CCC: $33.50
Published on Web 07/29/2006

and white regions represent, for example, the OsO_4-stained polyisoprene (PI) and unstained polystyrene (PS) lamellar nanodomains across the grain boundary for the SI diblock copolymer, respectively. The gray regions resulted when the PS and PI lamella come in contact at the TGB. Although the lamellar nanostructures are rather simple ones, the TEM image could be thus complicated across the boundary. Both Nishikawa et al.[5] and Gido et al.[6] employed this kind of computer simulation to study the 3D morphology of the lamellar grain boundaries, and they both concluded that the orthogonally intersecting lamellar nanodomains formed the Scherk's first surface. Recently, the Sherk's first surface was also used to study the motion of the TGB in the presence of an external field by computer simulation.[13] However, in contrast to this conclusion, Duque and Schick proposed the linear stack of dislocations (LSD)[14] as a better model for the TGB than the Scherk's first surface,[15] while Kamien and Lubensky concluded that the TGB is not given by either the linear stack of dislocations or Scherk's first surface.[16] In addition, Gido et al. proposed the "helicoid section boundary" for the TGB with low twist angles.[17] Thus, the morphology of the TGB is still a controversial issue.

Such a controversy about the TGB morphology arises partly from the lack of appropriate experimental techniques for 3D real-space volume imaging. Although TEM micrographs are real-space images of the grain boundary structures, they are not always conclusive because (i) they are 2D projections of 3D morphologies and (ii) the orientation of the grain boundary in the ultrathin section varies indefinitely, giving rise to a variety of patterns. To overcome such difficulties, as mentioned above, a computer simulation program to generate projections of 3D structures with an arbitrary thickness and orientation has been developed and used together with the TEM micrographs.[5,6] In such an analysis, however, the choice of the model surface becomes critical. Without an appropriate model, no analytical work would be carried out in this way. Therefore, it would be preferable to *directly* observe the grain boundary structures.

Transmission electron microtomography (TEMT) allows one to obtain a 3D image of the structural object[18] and, after an appropriate image analysis, to evaluate its structural parameters.[19] Block copolymer microphase-separated structures have been studied in 3D by TEMT,[20−24] some of which quantitatively characterized complex morphologies to evaluate their structural parameters from 3D digital data.[22,24] Recently, an improved 3D visualization technique, e.g., dual-axis electron tomography, for anisotropic nanostructures, e.g., cylinders, was demonstrated.[25]

In the present study, we take full advantage of the TEMT to study the grain boundary morphologies of a lamellar-forming block copolymer. We are particularly concerned with the grain boundary between two sets of lamellae that orthogonally intersect, i.e., the TGB morphology.

II. Experimental Section

A. Materials. Poly(styrene-*block*-isoprene) (SI) was purchased from Polymer Source, Inc., Canada. The number-average molecular weight (M_n) of the PS and PI blocks was 45 000 and 46 000, respectively. The volume fraction of PI in the SI copolymer was 0.54. The polydispersity index (PDI), M_w/M_n, for the diblock copolymer was 1.07. The molecular weight and PDI were determined by size exclusion chromatography. The block copolymer composition was calculated from the ^{1}H NMR spectra by comparing the peak area of the vinyic isoprene proton with the aromatic protons of polystyrene.

B. Specimens. A film specimen was prepared by casting from a ca. 5 wt % toluene solution. The cast film was annealed at 140 °C for 24 h under vacuum, which was subsequently stained by exposing the film to osmium tetraoxide (OsO_4) vapor for 1 day. The stained film thus obtained was ultramicrotomed with a diamond knife at room temperature using a Lica Ultracut UCT. The ultrathin section of ca. 190 nm thick was transferred onto a Cu mesh grid with a polyvinylformal substrate. Prior to the TEMT observation, 5 nm Au nanoparticles were deposited from an aqueous suspension (GCN005, BBInternational, Ltd., UK) and then coated with a thin layer of evaporated carbon to promote specimen stability under the electron beam.

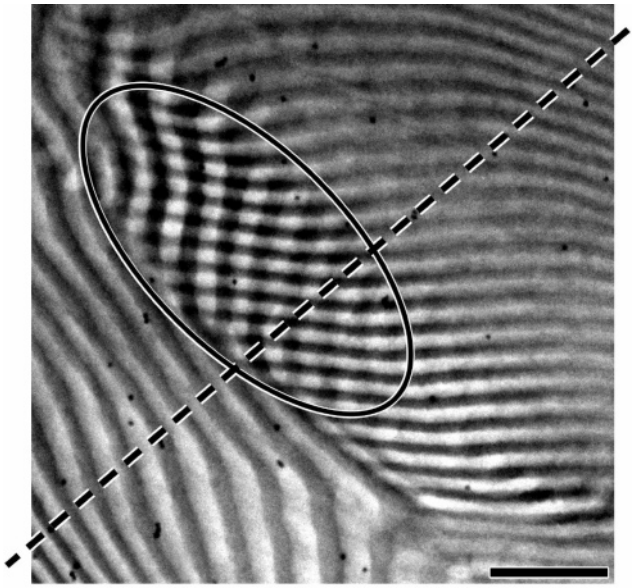

Figure 2. TEM micrograph of SI diblock copolymer. Black and white domains correspond to PI and PS nanodomains, respectively. The dashed line represents an axis around which the region marked by the ellipsoid was tilted. Small dots are Au nanoparticles (diameter: 5 nm). Bar indicates 200 nm.

C. Transmission Electron Microtomography. TEMT experiments were performed using an energy-filtering transmission electron microscope with a field-emission gun operated at 200 kV (JEM-2200FS, JEOL Co., Ltd., Japan). Projections were collected with a slow-scan CCD camera (Gatan USC1000, Gatan, Inc.). Note that only the transmitted and elastically scattered electrons (electron energy loss of 0 ± 15 eV) were selected by an in-column energy filter installed in the JEM-2200FS (Omega filter, JEOL, Ltd., Japan) in order to obtain achromatic projections. A series of TEM images were acquired at tilt angles ranging from $-60°$ to $+56°$ at the angular interval of 1°. Subsequently, the tilt series of the TEM images (117 images) were aligned by the fiducial marker method[26] with the Au nanoparticles as the fiducial markers and then reconstructed on the basis of the filtered-back-projection (FBP) method.[27] All reconstruction procedures were carried out using software developed in our laboratory.

III. Results and Discussion

Figure 2 shows a TEM micrograph of the SI diblock copolymer. As marked by an ellipsoid, a crosshatched region characteristic of the TGB [see Figure 1b, top left ($\phi = 0°$) and top right ($\phi = 10°$)] was observed. This region was tilted to take a series of projections for the 3D reconstruction. We note here that the direction of the tilt axis has to be carefully chosen because anisotropic morphologies, e.g., lamellar and cylindrical nanostructures, will not be properly reconstructed into a 3D image under a particular experimental condition.[25] Namely, if the lamellar nanostructure lies perpendicular to the tilt axis, due to the limitation of the angular range available in the TEMT experiments, the nanodomains will not appear in the resulting 3D image. One of the best solutions to this problem is to employ two (orthogonal) tilt axes in the same area of the specimen.[25]

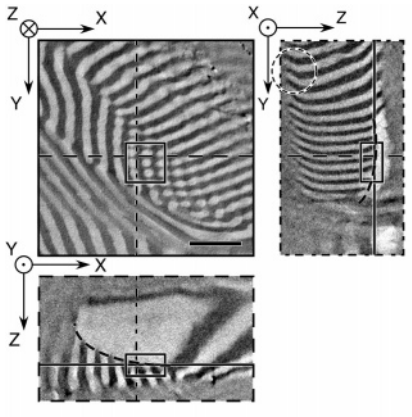

Figure 3. Orthogonal views of 3D reconstruction of SI diblock copolymer. *Z* axis is parallel to the depth direction of the ultrathin section. Dashed and solid lines in each cross section represent position of two other orthogonal cross sections. Bold curved dashed line in *X*−*Z* and *Y*−*Z* planes denotes grain boundary. Region marked by a rectangular solid will be binarized and shown later in Figure 5. Dashed circle in *Y*−*Z* plane indicates the effect of compressive force during microtomy. Bar indicates 200 nm.

Although such a "dual-axis tomography" offers a complete reconstruction with a much improved contrast, it is practically very demanding. Thus, in the present study, the tilt axis was chosen so that it had an angle of ca. 45° to the lamellar nanodomains in the crosshatched region.

An orthogonal cross-sectional view of the 3D reconstruction of the crosshatched region is shown in Figure 3. Each figure consists of three parts, i.e., the lateral plane (*X*−*Y* plane) and the *X*−*Z* and *Y*−*Z* planes. The FBP calculation was performed in the *X*−*Z* plane. The solid and dashed lines in each cross-sectional slice represent positions of the other two orthogonal slices. Note that the thickness of the three cross sections in Figure 3 is equal to the edge length of a voxel, i.e., 1.4 nm. Thus, in contrast to the conventional TEM micrograph as shown in Figure 2, the images were much clearer due to essentially no overlap of the nanostructure. We hereafter call the cross-sectional slice a "digital slice".

In the orthogonal cross sections shown in Figure 3, the soptlike nanopattern (marked by a rectangle in the *X*−*Y* plane) corresponded to the grain boundary region. The upper and lower lamellar grains were almost parallel to the *X*-axis and *Y*-axis, respectively (see *X*−*Z* plane, for example). Thus, the two grains almost orthogonally intersected in this region. Moreover, as indicated by the dashed bold lines in the *X*−*Z* and *Y*−*Z* planes, the boundary was found to be a curved, not a flat plane, contradicting the predicted or assumed model in the earlier studies, i.e., the Scherk's first surface.[5,6,12] In addition, since we did not observe sharp bending of lamellae and sudden change in lamellar periodicity in *X*−*Z* and *Y*−*Z* planes except for the very surface of the section (see for example the dashed circle in the *Y*−*Z* plane in Figure 3), we consider that the effect of microtomy that imposes (compressive) force was not significant in the interior of the section.

Prior to the structural analysis, it is necessary to find an interface between the PS and PI nanodomains; therefore, the *X*−*Y* digital slice at different *Z* values was binarized as demonstrated in Figure 4. Part a of the figure is the same *X*−*Y* digital slice as shown in Figure 3, while the corresponding binarized version is shown in part b. The threshold value used for the binarization is indicated by the arrow in the histogram (see Figure 4c). Note that the original digital slice had a strong contrast between the two domains, and hence the histogram

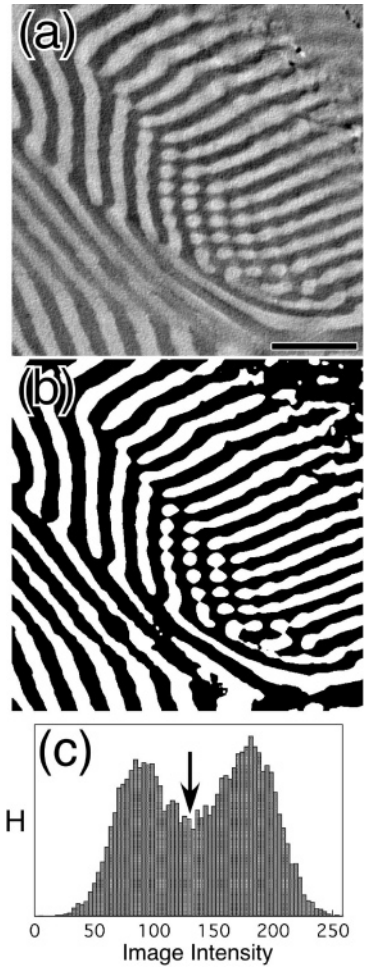

Figure 4. An *X*−*Y* digital slice at different depths in the 3D reconstruction of SI diblock copolymer (a) was binarized to find interface between PI and PS nanodomains (b). The threshold is indicated by an arrow in the histogram (c). Bar indicates 200 nm.

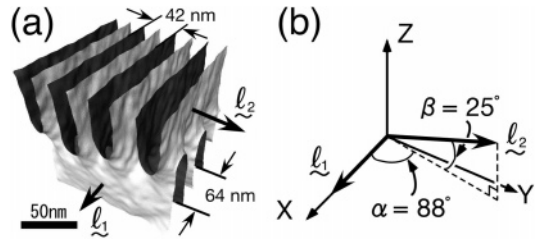

Figure 5. (a) Surface-rendered 3D image of grain boundary in SI diblock copolymer. The rectangular solid shown in Figure 3 was reconstructed. The interface is colored gray on one side and white on the other. The nanodomain looking toward the gray side is the PI nanodomain, while the PS nanodomain is toward the white side. Lamellar normals of upper and lower grains are displayed by arrows. Tilt and twist angles between the two lamellar grains are demonstrated in (b), in which the normal of the lower lamella, ℓ_1, lies along the *X*-axis.

exhibited bimodal peaks, which allowed us to determine the interface with high accuracy. After binarizing the *X*−*Y* planes at different depth positions, they were stacked to generate a binarized 3D reconstructed image. The marching cubes algorithm[28] that gives a triangular representation of the surface was employed.

Depicted in Figure 5a is the 3D surface-rendered image reconstructed from the region displayed in the rectangle in Figure 3a. The TGB was clearly demonstrated. The upper and lower lamellar nanodomains almost perpendicularly intersect.

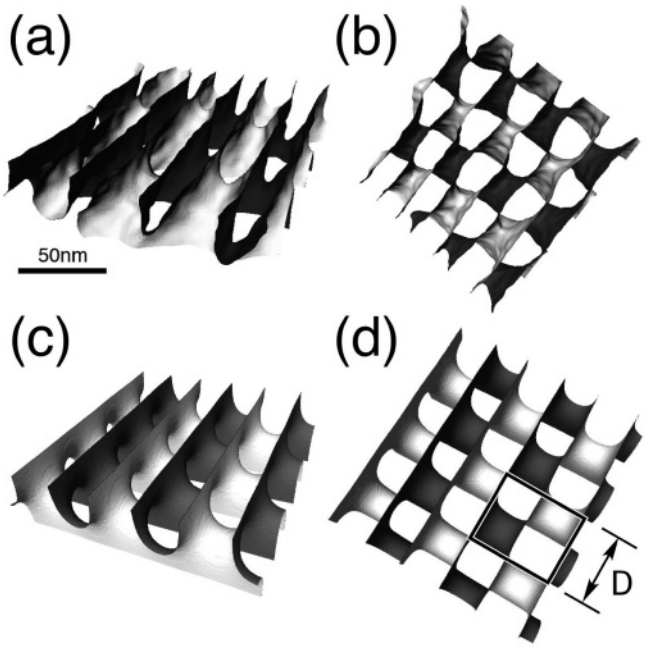

Figure 6. Experimentally observed grain boundary of SI diblock copolymer viewed from (a) side and (b) top. Corresponding Scherk's first surfaces are shown in (c) and (d). In (d), unit cell viewing from the top is shown by the bold boxed region.

The 3D Fourier transformation (FT) was separately carried out in the upper and lower lamellar domains to calculate the structure factors of the domains. The "diffraction spots" of the structure factors were used to determine the lamellar normals, which are schematically shown by $\not{1}$ and $\not{2}$ in Figure 5. $\not{2}$ is aligned with the *X*-axis. The twist angle, α, was found to be 88°. The tilt angle, β, was 25°. Note that the ideal TGB has $\beta = 0°$. Thus, rigorously speaking, the grain boundary observed here was *not* a perfect TGB, but yet it may be within the TGB category, at least in an experimental sense. The term "tilt angle" of the TGB may be confused with the "tilting angle" (of the specimen) in the TEMT experiments. Thus, we hereafter call the latter the "rotation angle".

In Figure 5, it is quite intriguing that the lamellar spacing, *D*, of the upper and lower nanodomains were found to be 42 and 64 nm, being different by a factor of ca. 50%, probably due to the local strain field on the lamellar periodicity near the boundary. According to the literature,[29] the domain spacing of the SI block copolymer used in this study should be around 50 nm. We note here that, even in the interior of the grains, a significant distribution of lamellar spacing was observed in our SI diblock coplymer system.[30]

Let us now compare the experimentally obtained TGB with the Sherk's first surface. Parts a and b of Figure 6 show the TGB obtained by the TEMT viewed from two different angles, while parts c and d are the computer-generated Scherk's first surfaces on the basis of eq 1 from similar directions as in Figure 6a,b. On the basis of these figures, the observed TGB appeared to be quite similar to the Scherk's first surface (see especially Figure 6b,d).

To *quantitatively* investigate whether the grain boundary of the TGB truly is the Scherk's first surface, the interfacial curvatures of the grain boundary were measured according to the same protocol as described elsewhere.[19,31,32] The area-averaged curvatures were measured at the experimentally obtained TGB of the SI copolymer (Figures 6a and 6b) and the model surface of the Scherk's first surface (Figures 6c and 6d). In the model surface, *D* was set to 53.4 nm, an average value for the two lamellar spacings experimentally observed at the grain boundary. Note that the grain boundary width was *D* in both cases.

Table 1. Surface Curvatures and Surface Area of Grain Boundary

	SI copolymer (TEMT)	Scherk's surface (model)	Scherk's surface (prediction)	LSD[a] (model)
angular range (deg)	−60 to 56	−60 to 56		−60 to 56
$\langle H \rangle (D^{-1})$	0.26 ± 0.01	0.039	0	0.070
$\langle K \rangle (D^{-2})$	−3.9 ± 0.1	−6.5	−6.5	−9.0
$S/V (D^{-1})$	2.4 ± 0.1	2.26	2.2	2.37

[a] Linear Stack of Dislocation.[16] *D* represents lamellar spacing.

In the interfacial curvature measurements, the roughness of the surface of the 3D reconstruction *significantly* affects the accuracy of the measurements. An index termed "roughness index (RI)", which provides a measure of the roughness of the surface constructed by triangles relative to the averaged curvatures, was used to characterize the quality of the surface.[31] The smaller the RI, the smoother the constructed surface. The index was 0.042 and 0.043 for the grain boundaries of the SI copolymer and of the Scherk's surface model, respectively. In other words, the model surface was made so that it had a surface quality similar to the experimental data. To make a fair comparison between the model and experimental results, we constructed the model surface in exactly the same manner as we reconstructed the TGB of the SI copolymer. Namely, the projections of the Scherk's first surface at the (experimentally used) angular range, i.e., −60° to 56°, were first simulated, which were then used to reconstruct the models Scherk's surface. Such a tedious protocol was necessary because there exists an undesirable elongation of the reconstructed 3D objects along the *Z*-axis due to the incomplete rotation.[33,34] Note that the CT requires a complete rotation, i.e., a ±90° tilting of the specimen.

Table 1 lists the area-averaged mean curvature, $\langle H \rangle$, Gaussian curvature, $\langle K \rangle$, and surface area per unit volume, *S*/*V*, in the grain boundary of the SI block copolymer and the Scherk's first model surface. The predicted values from the differential geometry are also listed in the table. Note that Table 1 also contains the curvatures and *S*/*V* of the LSD for reference. All the listed quantities are scaled by *D* for direct comparison. Let us first compare the Scherk's first surface with the prediction. A good agreement was found in the curvatures and *S*/*V*, demonstrating that the incomplete rotation of the TEMT experiments had only a slight effect on the curvature measurements in this case. We then examined the results of the SI block copolymer. *S*/*V* of the SI block copolymer showed a result similar to that of the model as well as that of the prediction. It was found that the TGB of the SI block copolymer had negative $\langle K \rangle$, suggesting that it belongs to the class having a hyperbolic surface. Since the Scherk's first surface is also the hyperbolic surface, this result is consistent with the previous hypothesis.[12] $\langle K \rangle$ of the SI copolymer was closer to the (predicted) value of Scherk's surface than that of the LSD.

A positive $\langle H \rangle$ was obtained for the SI copolymer. The absolute value is 1 order of magnitude larger than the $\langle H \rangle$ of either the Scherk's surface or the LSD. Since the difference in $\langle H \rangle$ between the model Scherk's first surface and the prediction was negligibly small, the elongation of the 3D image due to incomplete rotation (of the specimen) does not account for the difference. To make the discussion intuitive, the area-averaged principal radii were evaluated:[35] First, the averaged principal curvatures, $\langle k_1 \rangle$ and $\langle k_2 \rangle$, were estimated by solving the quadratic equation, i.e., $x^2 - 2\langle H \rangle x + \langle K \rangle = 0$, where the variable $x = \langle k_i \rangle$ ($i = 1$ or 2). The area-averaged radii were then estimated by taking the inverse of the principal curvatures: $\langle R_i \rangle \equiv$

$|1/\langle k_i \rangle|$ ($i = 1$ or 2).[35] The obtained area-averaged principal radii of the SI copolymer were 23.5 and −30.3 nm. Note that the sign of the radii is positive if the center of the osculating circle lies inside the PI nanophase. The difference in the two principal radii was ca. 7 nm, which corresponds to ca. 5 voxels. We consider that this difference would not be significant, since the experimentally obtained TGB of the SI copolymer was not an ideal one due to the following aspects: (i) The tilt angle, β, should be 0° for the ideal case, but was actually 25° (see Figure 5b), and (ii) lamellar spacings across the boundary were not identical. Therefore, roughly speaking, the difference in the two $\langle R \rangle$ values might be small enough to consider that they could be rather equal, meaning $\langle H \rangle$ may be regarded as zero. Therefore, the TGB of SI copolymer had the characteristic of the minimal surface, and hence the minimization of the surface area, i.e., the minimization of the surface energy, is the dominant cause of the structural formation as hypothesized earlier.[12] In addition, it seems that the Scherk's first surface may be a better model of the TGB than the LSD in our experiment.

As demonstrated in the present study, our experimental approach can provide information about the 3D grain boundary. At this moment, however, very few mathematical models have been proposed to account for the grain boundary except for a special case ($\alpha = 90°$ and $\beta = 0°$). For a complete understanding of the grain boundary morphologies, theoretical predictions or computer simulation works with various α and β values will be strongly required.

Acknowledgment. The authors are grateful to NEDO for supporting this study through the Japanese National Project "Nano Structured Polymer Project" by the Ministry of Economy, Trade and Industry. The authors are grateful to Dr. Y. Nishikawa and Mr. K. Niihara for his valuable discussions and comments.

References and Notes

(1) Hamley, I. W. *Developments in Block Copolymer Science and Technology;* John Wiley & Sons, Ltd: Chichester, 2004.
(2) Hamley, I. W. *Nanotechnology* **2003**, *14*, R39.
(3) Ehlich, D.; Takenaka, M.; Okamoto, S.; Hashimoto, T. *Macromolecules* **1993**, *26*, 189.
(4) Ehlich, D.; Takenaka, M.; Hashimoto, T. *Macromolecules* **1993**, *26*, 492.
(5) Nishikawa, Y.; Kawada, H.; Hasegawa, H.; Hashimoto, T. *Acta Polym.* **1993**, *44*, 247.
(6) Gido, S. P.; Gunther, J.; Thomas, E. L.; Hoffman, D. *Macromolecules* **1993**, *26*, 4506.
(7) Gido, S. P.; Thomas, E. L. *Macromolecules* **1994**, *27*, 849.
(8) Qiao, L.; Winey, K. I. *Macromolecules* **2000**, *33*, 851.
(9) Qiao, L.; Winey, K. I.; Morse, D. C. *Macromolecules* **2001**, *34*, 7858.
(10) Qiao, L.; Ryan, A. J.; Winey, K. I. *Macromolecules* **2002**, *35*, 3596.
(11) Matsen, M. W. *J. Chem. Phys.* **1997**, *107*, 8110.
(12) Thomas, E. L.; Anderson, D. M.; Henkee, C. S.; Hoffman, D. *Nature (London)* **1988**, *334*, 598.
(13) Kamien, R. D.; Lubensky, T. C. *Phys. Rev. Lett.* **1999**, *82*, 2892.
(14) The Scherk's first surface is a dilated surface of the LSD along the twist axis by $\cos(\alpha/2)$.[16] Since α is 90° for the TGB, the factor is $1/\sqrt{2}$.
(15) Duque, D.; Schick, M. *J. Chem. Phys.* **2000**, *113*, 5525.
(16) Kyrylyuk, A. V.; Fraaije, J. G. E. M. *Macromolecules* **2005**, *38*, 8546.
(17) Scherk, H. F. *Reine Angew. Mater.* **1835**, *13*, 185.
(18) Frank, J. *Principles of Electron Tomography*; Plenum Press: New York, 1992.
(19) Jinnai, H.; Nishikawa, Y.; Ikehara, T.; Nishi, T. *Adv. Polym. Sci.* **2004**, *170*, 115.
(20) Spontak, R. J.; Williams, M. C.; Agard, D. A. *Polymer* **1988**, *29*, 387.
(21) Radzilowski, L. H.; Carragher, B. O.; Stupp, S. I. *Macromolecules* **1997**, *30*, 2110.
(22) Jinnai, H.; Nishikawa, Y.; Spontak, R. J.; Smith, S. D.; Agard, D. A.; Hashimoto, T. *Phys. Rev. Lett.* **2000**, *84*, 518.
(23) Niihara, K.; Nishikawa, Y.; Nishi, T.; Jinnai, H. *Trans. Mater. Res. Soc. Jpn.* **2005**, *30*, 617.
(24) Nishioka, H.; Niihara, K.; Kaneko, T.; Nishikawa, Y.; Yamanaka, J.; Inoue, T.; Nishi, T.; Jinnai, H. *Compos. Interfaces*, in press.
(25) Sugimori, H.; Nishi, T.; Jinnai, H. *Macromolecules* **2005**, *38*, 10226.
(26) Lawrence, M. C. Least-squares method of alignment using markers. In *ELECTRON TOMOGRAPHY Thee-dimensional Imaging with the Transmission Electron Microscope*; Frank, J., Ed.; Plenum Press: New York, 1992.
(27) Crowther, R. A.; DeRosier, D. J.; Klug, A. *Proc. R. Soc. London* **1970**, *A317*, 319.
(28) Lorensen, W. E.; Cline, H. E. *Computer Graphyics, SIGGRAPH '87* **1987**, *21*, 163.
(29) Hashimoto, T.; Shibayama, M.; Kawai, H. *Macromolecules* **1980**, *13*, 1237.
(30) Jinnai, H.; Niihara, K.; Sawa, K.; Yasuda, K.; Nishi, T., manuscript in preparation.
(31) Nishikawa, Y.; Jinnai, H.; Koga, T.; Hashimoto, T. *Langmuir* **1998**, *14*, 1242.
(32) Nishikawa, Y.; Koga, T.; Hashimoto, T.; Jinnai, H. *Langmuir* **2001**, *17*, 3254.
(33) Kaneko, T.; Nishioka, H.; Nishi, T.; Jinnai, H. *J. Electron Microsc.* **2005**, *54*, 437.
(34) Kawase, N.; Kato, M.; Nishioka, H.; Jinnai, H. *Ultramicroscopy*, in press.
(35) Jinnai, H.; Koga, T.; Nishikawa, Y.; Hashimoto, T.; Hyde, S. T. *Phys. Rev. Lett.* **1997**, *78*, 2248.

MA0600153